

Local structure of ionic solid solutions: Extended x-ray absorption fine-structure study

J. B. Boyce and J. C. Mikkelsen, Jr.

Xerox Palo Alto Research Center, Palo Alto, California 94304

(Received 19 February 1985)

The first-neighbor distances in the ionically bonded rocksalt-structured solid solutions $(K_{1-x}Rb_x)Br$ and $Rb(Br_{1-x}I_x)$ differ substantially from the average, or virtual-crystal, distance. There is, nonetheless, a significant variation in the first-neighbor distances with composition, indicating that the Pauling concept of the conservation of ionic radii is not valid. This change, relative to the change in the lattice constant, is about twice as large as that observed in covalently bonded, zinc-blende-structured solid solutions, resulting from the different crystal structures for these two alloy systems.

The local structural distortions around impurity atoms in alloys have, until recently, been outside the realm of direct experimental determination. Previously, they were inferred from their effects on the intensities of Bragg diffraction peaks and the associated diffuse scattering. Extended x-ray-absorption fine structure (EXAFS), on the other hand, provides a direct measure of the near-neighbor environment. Because of its spectroscopic and local nature, EXAFS is an ideal structural probe for determining the distortions of the host lattice in the vicinity of impurities in dilute binary alloys,¹⁻⁵ as well as the near-neighbor environment in ternary and quaternary solid solutions.⁶⁻¹⁰

We have recently used EXAFS to determine the local structural environment in solid solutions of $(Ga_{1-x}In_x)As$ over the entire composition range of x from 0 to 1.⁹ These alloys are covalently bonded semiconductors with the zinc-blende structure; they form random solid solutions over the entire composition range; and their lattice constant a_0 varies linearly with x ; i.e., it accurately follows Vegard's law. The EXAFS results on the K edges of each of the three constituent atoms indicate the following. (1) The first-neighbor distances r_1 remain closer to the respective distances in the pure binary compounds than to the average, or virtual-crystal, distance determined from the lattice constant of the alloy. There is, nonetheless, a change in r_1 with composition equal to 20% of the change in the average-crystal first-neighbor distance. (2) Despite the compositional disorder, there is no significant broadening in the width of the first-neighbor distribution in the alloys over that in the pure binary compounds. (3) The second-neighbor distribution indicates that the cation-cation distances are approximately equal to the average distance, whereas the anion-anion distribution is bimodal, with As-Ga-As and As-In-As distances close to those in GaAs and InAs, respectively. Very similar results were obtained for the anion-substituted, zinc-blende alloy $Zn(Se_{1-x}Te_x)$.

The question then arises as to how these results may differ in crystals with a different structure and local bonding. For example, a specific question is whether the near conservation of the first-neighbor distance observed in $(Ga_{1-x}In_x)As$ is typical of pseudobinary alloys or is a result of the strong covalent bonding in this material. To address these issues, we have performed similar EXAFS experiments on the ionically bonded, rocksalt-structured alloys $(K_{1-x}Rb_x)Br$ and $Rb(Br_{1-x}I_x)$. We have chosen these systems since the local structural distortions in ionic solid solutions might be expected to differ substantially from those in

covalently bonded alloys due to the differences in the crystal structure and in the nature of the bonding. The covalent bond is strong, directional, and allows for tetrahedral (fourfold) coordination. The ionic bond is central, with Coulomb and softened-hard-sphere interactions, and allows for octahedral (sixfold) coordination. In addition, the various elastic constants tend to decrease with increasing ionicity.

Despite the differences in the nature of the bonding and the lattice structure, the local structural results for these ionic pseudobinary alloys are remarkably similar to those for their covalent counterparts. The first-neighbor distances are very different from the average, or virtual-crystal, distance of the alloy, and the widths of those distributions are not substantially larger than those for the pure binary compounds. The second-neighbor cation-cation distribution for cation-disordered $(K_{1-x}Rb_x)Br$ is also similar to that in $(Ga_{1-x}In_x)As$ in that it is approximately equal to the average distribution, although it is broader. The anion-anion second-neighbor distribution does differ but in a manner consistent with the difference in the two crystal structures. A similar comparison of the second-neighbor distributions can be made for the anion-substituted alloys $Rb(Br_{1-x}I_x)$ and $Zn(Se_{1-x}Te_x)$. Concerning the ionic-versus-covalent issue, the major difference is that the first-neighbor distances vary more with composition for the ionic alloys than for the covalent ones. This difference is mainly a function of the different crystal structures, which result from the different types of bonding for the two systems.

Polycrystalline solid solutions of $(K_{1-x}Rb_x)Br$ and $Rb(Br_{1-x}I_x)$ for $x=0, 0.02, 0.1, 0.25, 0.5, 0.75, 0.9,$ and 1.0 were made by melting appropriate mixtures of high-purity $KBr, RbBr,$ and RbI , followed by repeated grinding and sintering within $25^\circ C$ of the alloy solidus temperature. X-ray powder diffraction was used to monitor the degree of homogeneity. The EXAFS samples were prepared by mixing fine powders with epoxy and spreading to achieve a thickness of about two absorption lengths above the K edge of interest ($\sim 75 \mu m$ thick). Transmission x-ray photographs were used to verify that the samples were homogeneous and free from pin holes. The EXAFS spectra for each sample were obtained at 77 and 300 K on the Rb, Br, and I K -shell absorption edges using a wiggler side station at the Stanford Synchrotron Radiation Laboratory. The data were collected in the transmission mode and were reduced and analyzed in real space, using standard techniques.¹¹ The binary end-point compounds served as structural standards. The first-neighbor and second-neighbor structural in-

formation, i.e., the number and type of each neighboring atom, its mean near-neighbor distance, and the distribution (width) about the mean, were determined using least-squares fits to the data in real space.

Figure 1 shows an example of the EXAFS on the Rb *K*-edge transformed to real space for pure RbBr and 2 mol% RbBr in KBr. The first peak in each case corresponds to the six Br first neighbors to the central Rb ion, the second peak to the cation second neighbors, and so on. From this figure, two results are immediately evident. First, the Br first-neighbor peaks in each case are almost identical in shape and phase, with only a small relative shift in position. This indicates that the Rb ion in the alloy occupies a substitutional *K* site with six Br first neighbors, as expected, but with a somewhat shorter Rb-Br first-neighbor distance ($\Delta r_1 = -0.06$ Å) than in pure RbBr. Secondly, the further neighbor peaks are altered in the alloy due to the cation-sublattice disorder. The second-neighbor peaks in Fig. 1 correspond to 12 Rb atoms in the pure RbBr case but to almost 12 K atoms in the $(\text{Rb}_{0.02}\text{K}_{0.98})\text{Br}$ case (for a random solid solution, 11.8 K and 0.2 Rb). This data indicate that good mixing of the constituent atoms occurs, with no significant clustering, even on a distance scale of the second neighbors.

The results on the first-neighbor distances, r_1 , in $(\text{K}_{1-x}\text{Rb}_x)\text{Br}$ determined in least-squares fits to the data for the various alloy compositions are shown in the upper portion of Fig. 2. It is seen that $r_1(\text{Rb-Br})$ and $r_1(\text{K-Br})$ differ substantially from one another and from the virtual-crystal distance. The variations in r_1 with alloy composition are more substantial than those for $(\text{Ga}_{1-x}\text{In}_x)\text{As}$ and $\text{Zn}(\text{Se}_{1-x}\text{Te}_x)$. But as in the covalent case, the widths of

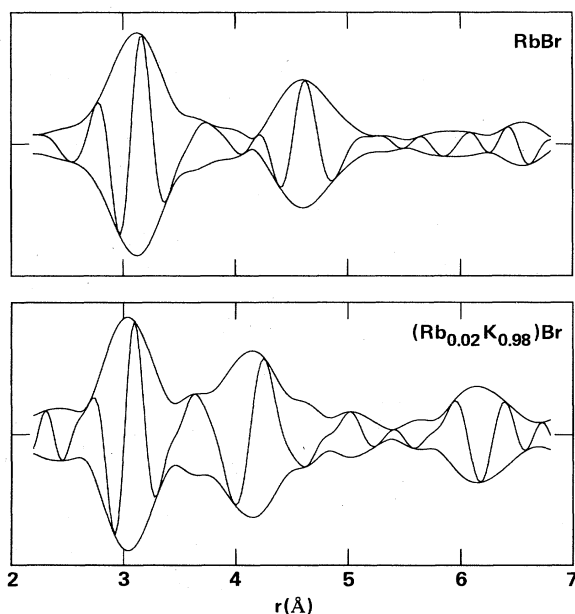


FIG. 1. Real part and the magnitude (envelope curve) of the Fourier transform of k times the EXAFS, $\chi(k)$, on the Rb *K* edge of pure RbBr (upper drawing) and the alloy $(\text{Rb}_{0.02}\text{K}_{0.98})\text{Br}$ (lower drawing), both at 77 K. The data were transformed using a square window $\text{fofm } k=2$ to 16 \AA^{-1} , broadened by a Gaussian of half-width 0.7 \AA^{-1} .

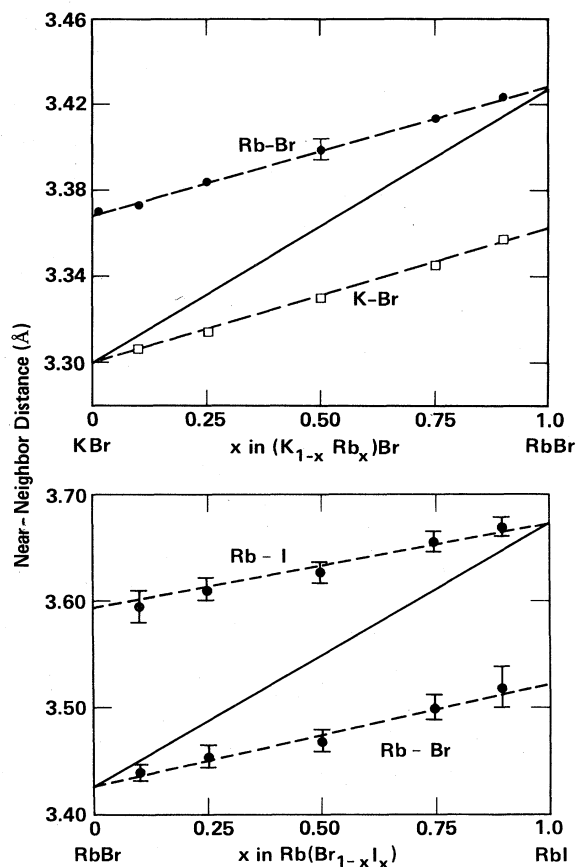


FIG. 2. (Upper drawing) Rb-Br and K-Br first-neighbor distances as a function of alloy composition in $(\text{K}_{1-x}\text{Rb}_x)\text{Br}$. The middle curve is the virtual-crystal approximation (VCA) cation-anion bond length obtained from Vegard's law. The weighted average of the first-neighbor distances agrees with the VCA average. (Lower drawing) Rb-I and Rb-Br first-neighbor distances in $\text{Rb}(\text{Br}_{1-x}\text{I}_x)$.

the first-neighbor peaks are not substantially larger than those for the pure binary compounds used as structural standards. This argues against a large variation in r_1 at a specific alloy composition due to the local compositional disorder. Similar first-neighbor results are obtained for the anion-disordered alloy $\text{Rb}(\text{Br}_{1-x}\text{I}_x)$, also shown in Fig. 2.

The second-neighbor distribution is more complex in $(\text{K}_{1-x}\text{Rb}_x)\text{Br}$ and in $\text{Rb}(\text{Br}_{1-x}\text{I}_x)$ than in the covalent materials, due to the higher coordination number. In $(\text{Ga}_{1-x}\text{In}_x)\text{As}$, for example, two As anions are bonded together via one cation only, so the obtained bimodal distribution of As second-neighbor distances, corresponding to the two types of intervening cations, is readily understood. In $(\text{K}_{1-x}\text{Rb}_x)\text{Br}$, however, two Br anions are bonded via two cations. Thus, three possibilities exist in this octahedral case, rather than two as in the tetrahedral case: Br-(K,K)-Br, Br-(Rb,Rb)-Br, and Br-(K,Rb)-Br. From the data, a single Br-Br-peak can indeed be ruled out. But owing to a finite signal-to-noise ratio and some peak overlap, the data were not adequate to distinguish between two Br-Br peaks or three Br-Br peaks, and reliably determine the corresponding structural parameters. Both a two-peak and a three-peak distribution gave good fits to the data. All that could be

determined reliably is that the second-neighbor Br-Br distribution is consistent with a three-peak distribution corresponding to the three different configurations. Consider, for example, the results on $(K_{0.5}Rb_{0.5})Br$. A three-Gaussian fit gave an excellent fit with three Br-Br pairs at 4.85 Å, three at 4.67 Å, and six at 4.75 Å. These results yield the correct number of different pairs of neighbors for a random solid solution and the distances are within 0.01 Å of what one would expect from the Br-Br distances in the end-point compounds: 4.847 Å for Br-(Rb,Rb)-Br, 4.667 Å for Br-(K,K)-Br, and half way in between (4.757 Å) for Br-(K,Rb)-Br.

The cation-cation distribution in $(K_{1-x}Rb_x)Br$, on the other hand, was determined to be a single broad peak, as in the $(Ga_{1-x}In_x)As$ case, located at the virtual-crystal second-neighbor distance. The number of K and Rb second neighbors to a Rb central atom are approximately $12(1-x)$ and $12x$, respectively, indicating that this system forms a good random solid solution. For $Rb(Br_{1-x}I_x)$, which has an anion rather than cation substitution, the second-neighbor situation is very similar to that in $(K_{1-x}Rb_x)Br$, with cation replaced by anion and vice versa. Thus, the fcc sublattice with the substitutional disorder retains an fcc array that changes size (lattice constant) as the composition is varied and is somewhat distorted giving rise to the broad width of the peak. The common-sublattice fcc array, on the other hand, undergoes a substantial local distortion in response to the different-sized ions substituted on the other sublattice.

The major difference between the first-neighbor distributions for the ionically bonded (rocksalt) versus covalently bonded (zinc-blende) alloys is that the variation of r_1 with alloy composition is larger for the ionic case. For the covalent alloys, the total variation in r_1 with composition, Δr_1 , is about 20% of the total variation in the virtual-crystal first-neighbor distance, Δr_{1v} .¹² In the ionic case, it is about 40% [from Fig. 2 it is about 45% for $(K_{1-x}Rb_x)Br$ and 35% for $Rb(Br_{1-x}I_x)$]. A similar large variation of 40% has been observed in the fluorite-structured alloy Sr-doped CaF_2 .¹⁰ The larger variation for the ionic solid solutions is in reasonable agreement with a prediction from the recent calculations of Shih, Spicer, Harrison, and Sher,¹³ using a simple radial force model. Their model assumes that only the bond-stretching force constants are important, with the bond-bending forces being ignored. They also assume that the common sublattice (e.g., Br) is the one that distorts in

response to the different-sized impurity atom on the sublattice with substitutional disorder (e.g., K and Rb), which is assumed to remain fixed. (This is quite close to what is observed experimentally, as discussed above.) From this simple model they predict $\Delta r_1/\Delta r_{1v} = \frac{1}{2}$ for alloys with the rocksalt structure (compared with the experimental value of about 0.4) and $\Delta r_1/\Delta r_{1v} = \frac{1}{4}$ for alloys with the zinc-blende structure (compared with the experimental value of 0.2). The different results for the two crystal structures is due merely to geometry, i.e., octahedral versus tetrahedral coordination. This implies that the larger distortions observed in the ionically bonded alloys compared with those in the covalently bonded alloys is directly due to their different crystal structure, which, in turn, results from the different nature of the bonding.

In addition, the experimental values of r_1 for the ionic solid solutions are in approximate agreement with the more rigorous and detailed calculations of Dick and Das¹⁴ using a Born-Mayer model on dilute solid solutions of alkali halides. Their conclusion is that the displacements of the host first neighbors about the impurity ion are about $\frac{1}{2}$ of the difference between the ionic radii of the unlike host and impurity ions. In other words, these calculations indicate that the change in the first-neighbor distance, Δr_1 , should be about 50% of the change in the virtual-crystal first-neighbor distance, Δr_{1v} . These calculations considered $Na(Cl,Br)$ and $(K,Na)Br$ rather than the two ionic solid solutions studied here. Nonetheless, the basic conclusion from these calculations might be expected to apply to $(K_{1-x}Rb_x)Br$ and $Rb(Br_{1-x}I_x)$. We observe a change of approximately 40%, consistent with this prediction of 50%.

In summary, the first-neighbor distances in ionically bonded rocksalt-structured solid solutions differ substantially from the average, or virtual-crystal, distance. There is, nonetheless, a significant variation in the first-neighbor distances with composition. This change is about twice as large as that observed in covalently bonded zinc-blende-structured solid solutions, resulting from the different crystal structures of these two alloy systems.

We wish to acknowledge helpful discussions with C. Herring. The Stanford Synchrotron Radiation Laboratory is supported by the Department of Energy and the National Institute of Health.

¹A. Fontaine, P. Lagarde, A. Naudeon, D. Raoux, and D. Spanjaard, *Philos. Mag.* B 4, 17 (1979).

²T. M. Hayes, J. W. Allen, J. B. Boyce, and J. J. Hauser, *Phys. Rev.* B 22, 4503 (1980).

³D. Raoux, A. Fontaine, P. Lagarde, and A. Sadoc, *Phys. Rev.* B 24, 5547 (1981).

⁴J. Mimault, A. Fontaine, P. Lagarde, D. Raoux, A. Sadoc, and D. Spanjaard, *J. Phys.* F 11, 1311 (1981).

⁵B. Lengeler and P. Eisenberger, *Phys. Rev.* B 21, 4507 (1980).

⁶J. B. Boyce and K. Baberschke, *Solid State Commun.* 39, 781 (1981).

⁷J. B. Boyce, R. M. Martin, J. W. Allen, and F. Holtzberg, in *Valence Fluctuations in Solids*, edited by L. M. Falicov, W. Hanke, and M. B. Maple (North-Holland, Amsterdam, 1981), p. 427.

⁸J. Azoulay, E. A. Stern, D. Shaltiel, and A. Grayevski, *Phys. Rev.* B 25, 5627 (1982).

⁹J. C. Mikkelsen, Jr. and J. B. Boyce, *Phys. Rev.* B 28, 7130 (1983).

¹⁰S. P. Vernon and M. B. Stearns, *Phys. Rev.* B 29, 6968 (1984).

¹¹T. M. Hayes and J. B. Boyce, in *Solid State Physics*, edited by H. Ehrenreich, F. Seitz, and D. Turnbull (Academic, New York, 1982), Vol. 37, pp. 173-351.

¹²J. B. Boyce and J. C. Mikkelsen, Jr., in *EXAFS and Near Edge Structure III*, edited by K. O. Hodgson, B. Hedman, and J. E. Penner-Hahn (Springer-Verlag, Berlin, 1984), p. 426.

¹³C. K. Shih, W. E. Spicer, W. A. Harrison, and A. Sher, *Phys. Rev.* B 31, 1139 (1985).

¹⁴B. G. Dick and T. P. Das, *Phys. Rev.* 127, 1053 (1962).